Diverse small-molecule modulators of SMN expression found by high-throughput compound screening: early leads towards a therapeutic for spinal muscular atrophy

Jill Jarecki[1,*], Xiaocun Chen[1], Alexandra Bernardino[1], Daniel D. Coovert[4], Michael Whitney[1,†], Arthur Burghes[2,3,4], Jeffrey Stack[1] and Brian A. Pollok[1,‡]

[1]Vertex Pharmaceuticals, Inc., 11010 Torreyana Road, San Diego, CA 92121, USA and [2]Department of Molecular Genetics, College of Biological Sciences, [3]Department of Neurology, College of Medicine and [4]Department of Molecular and Cellular Biology, Ohio State University, Columbus, OH 43210, USA

We have exploited the existence of a second copy of the human *SMN* gene (*SMN2*) to develop a high-throughput screening strategy to identify potential small molecule therapeutics for the genetic disease spinal muscular atrophy (SMA), which is caused by the loss of the *SMN1* gene. Our screening process was designed to identify synthetic compounds that increase the total amount of full-length SMN messenger RNA and protein arising from the *SMN2* gene, thereby suppressing the deleterious effects of losing *SMN1*. A cell-based bioassay was generated that detects *SMN2* promoter activity, on which greater than 550 000 compounds was tested. This resulted in the identification of 17 distinct compounds with confirmed biological activity on the cellular primary assay, belonging to nine different structural families. Six of the nine scaffolds were chosen on the basis of their drug-like features to be tested for their ability to modulate *SMN* gene expression in SMA patient-derived fibroblasts. Five of the six compound classes altered SMN mRNA levels or mRNA splicing patterns in SMA patient-derived fibroblasts. Two of the compound classes, a quinazoline compound series and an indole compound, also increased SMN protein levels and nuclear gem/Cajal body numbers in patient-derived cells. In addition, these two distinct scaffolds showed additive effects when used in combination, suggesting that they may act on different molecular targets. The work described here has provided the foundation for a successful medicinal chemistry effort to further advance these compounds as potential small molecule therapeutics for SMA.

INTRODUCTION

Proximal spinal muscular atrophy (SMA) is an autosomal recessive disease that is the leading hereditary cause of mortality in infants under the age of two (1). Approximately one in 8000 live births is afflicted with SMA, and the associated carrier rate is one in 40 to 50 individuals (2–4). This disease is characterized by the degeneration of the anterior horn cells of the spinal cord. The loss of the alpha-motor neurons results in progressive muscle atrophy and eventual paralysis and death.

SMA is caused by mutations, predominately gene deletions, in the telomeric copy of the survival of motor neuron gene (*SMN1*) on chromosome 5q13 (5). A second centromeric copy of the SMN gene (*SMN2*) also exists on chromosome 5, and both copies of the gene can produce functional protein (5). However, because of a single point mutation in exon 7 of the *SMN2* gene, 80% of *SMN2* transcripts lack exon 7

*To whom correspondence should be addressed at: Families of SMA, Libertyville, IL 60048, USA. Email: jill@fsma.org
†Present Address: University of California at San Diego, 9500 Gilman Dr, La Jolla, CA 92093, USA.
‡Present Address: Invitrogen Corporation, 501 Charmany Drive, Madison, WI 53719, USA.

(termed the Δ7 transcript) (6,7). In contrast, the transcripts arising from the *SMN1* gene typically include exon 7 (the full-length transcript). The absence of exon 7 from the SMN transcript results in mutated SMN protein with reduced ability for self-oligomerization, leading to protein instability and degradation (8,9). Thus, SMA patients have low SMN protein levels that are insufficient for motor neuron survival (10,11). The single point mutation in *SMN2* exon 7, resulting in the aberrant *SMN2* splicing pattern, is thought to disrupt an exonic splicing enhancer and/or create a novel splicing silencer site (12–14). Overexpression of the SR-splicing factor Htra2-β which specifically binds exon 7 mRNA and overexpression of a several other *trans*-acting splicing factors which directly interact with Htra2-β1, such as hnRNP-G, Srp30c and RBM, promote the inclusion of exon 7 into the mRNA transcript during SMN gene splicing events (15,16).

The 294 amino acid full-length SMN protein is ubiquitously expressed and localizes to both the cytoplasm and the nucleus, where it exists as a component of a multi-protein complex (10,11). In the nucleus, SMN accumulates in structures such as gems and Cajal bodies, which in many cell types are co-localized (17,18). SMN is believed to be a master assembler of RNP complexes and is known to have a critical role in snRNP biogenesis (19–21). It has also been reported to influence several other cellular activities such as pre-mRNA splicing (22,23), transcription (24,25), ribosomal assembly (26,27) and apoptosis (28–30).

However, the causal function of SMN in SMA disease progression remains unclear. The selective loss of motor neurons in SMA could result from the disruption of a known SMN function or from a novel function specific to motor neurons. SMN is found in the axons of motor neurons of several animal species, and its reduction results in motor axon defects in zebrafish. Thus, the SMN complex might be required for the transport of mRNA into axons and synapses, allowing for localized translation of mRNA in axons (31–35). Whether axonal transport of mRNA is the SMN activity responsible for SMA disease progression remains to be demonstrated.

Direct evidence indicates that *SMN2* is a modifier gene for SMA disease severity. SMA arises from the loss of the *SMN1* gene, but disease severity correlates with the number of *SMN2* genes (human *SMN2* can be amplified and copy number varies in the general population) and the corresponding amount of SMN produced from these genes (4,36–38). The hypothesis that the clinical severity of SMA can be suppressed by increasing *SMN2* gene copy number is supported by transgenic mice studies (39–43). The introduction of one or two copies of the human *SMN2* gene into *SMN* knockout mice (mice have only the *SMN1* gene and lack the *SMN2* gene) rescues embryonic lethality and the mice develop Type I SMA-like symptoms (41,42). When possessing eight copies of the human *SMN2* gene, SMN protein expression reaches normal levels, and the mice appear to be unaffected by the *SMN* gene ablation (42). Therefore, increasing human *SMN2* gene expression during the appropriate time in development will likely reduce the clinical severity of SMA.

We have exploited the existence of the disease-modifying human *SMN2* gene to develop a small-molecule drug discovery strategy for SMA. Our compound screening campaign sought to identify synthetic compounds that increase the total amount of full-length SMN messenger RNA and protein arising from the human *SMN2* gene. Here, we describe the development of the primary cellular screening assay, the execution of the screening campaign and the analysis and profiling of the primary screening compound hits using a series of secondary cellular assays. The most promising compounds found during this effort increase functional SMN2 levels and currently form the foundation of an active medicinal chemistry program to advance these compounds into pre-clinical development as potential small molecule therapeutics for SMA.

RESULTS

Generation and validation of the SMN2 promoter assay

To identify small molecule compounds that increase SMN expression, we generated a SMN2 promoter βlactamase (BLA) reporter gene assay in the mouse motor neuron cell line NSC-34. The NSC-34 cell line, a hybrid between mouse spinal cord cells and a mouse neuroblastoma, was utilized because it exhibits characteristics of motor neurons (44). A motor neuron-like cell type was preferred for assay development because SMA clinically presents only in motor neurons, even though SMN expression is ubiquitous and is known to possess an essential cellular function. In our assay, a 3.4 kb DNA fragment from the *SMN2* gene was used to drive BLA gene transcription. This fragment was previously shown to contain both positive and negative *cis*-regulatory elements that control *SMN2* gene transcription, allowing for the detection of synthetic compounds with two distinct mechanisms—increasing gene expression or relieving gene repression (45,46). Clonal cell lines were established using a flow cytometry selection strategy (described in Material and Methods) that enables the isolation of cells with low basal levels of BLA reporter gene expression. The resulting cell lines were screened for increased BLA activity after stimulation with the non-selective histone deacetylase (HDAC) inhibitors Trichostatin A and sodium butyrate, which are known to increase the transcription of 2% of all genes (47,48), including *SMN* (49). A fluorescent substrate of BLA named CCF2/AM, which emits 530 nM light when intact and 460 nM light when cleaved by BLA, was used to assess BLA activity by measuring the ratio of 460 to 530 nM emissions (see the Materials and Methods for details) (50,51). The single clonal cell line, selected as the SMN2 promoter assay, exhibited a 2-fold increase in BLA activity (the largest observed among the clones analyzed) in the presence of Trichostatin A and sodium butyrate (Fig. 1). The observed EC_{50} values of these two compounds in the promoter assay were consistent with those described in the literature. The non-sigmoidal nature of the dose response curves of these compounds is due to cellular toxicity induced at concentrations at or just above the maximal effective dose. After assay optimization, which included determining optimal serum levels, plating density and compound incubation time, the promoter assay was shown to display the dynamic range and reproducibility required for a
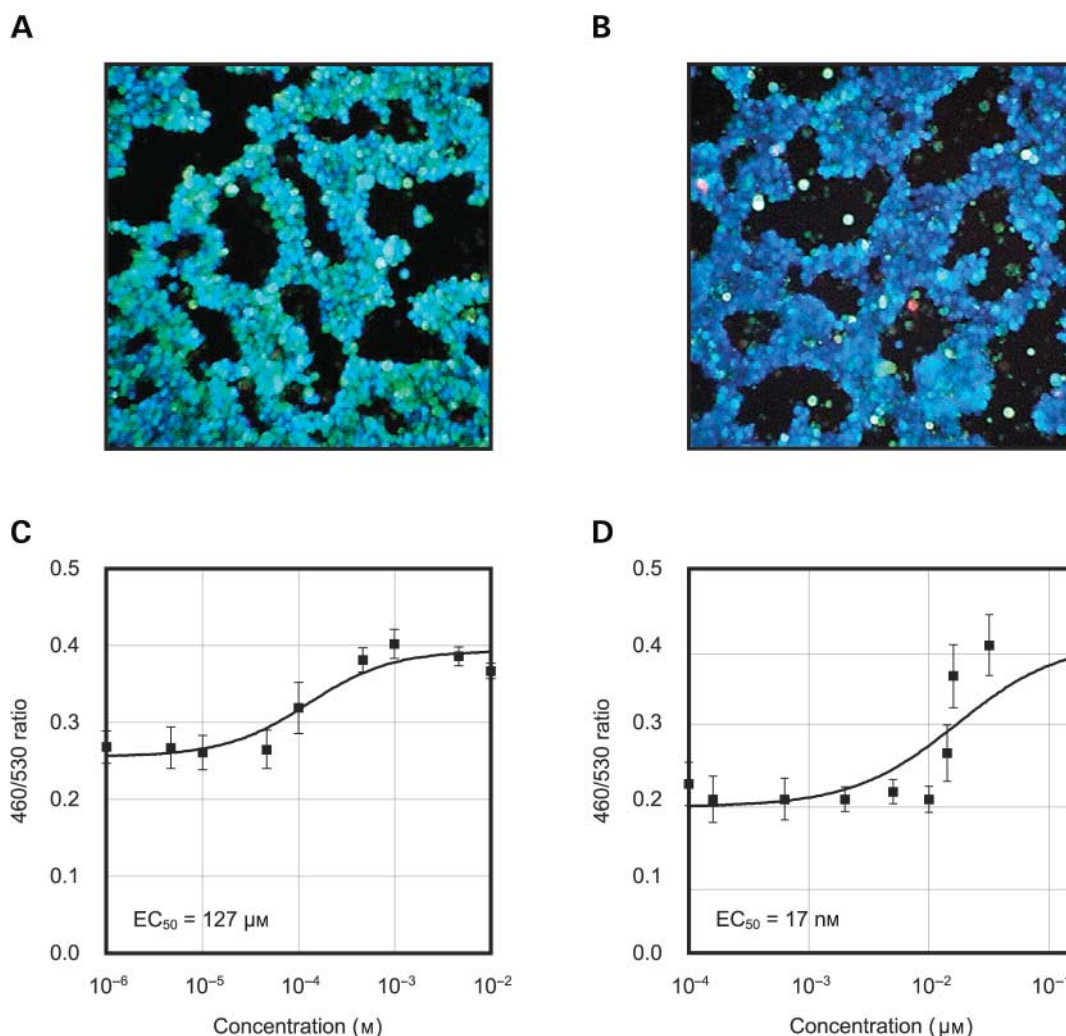
A

B

C

D

Figure 1. BLA response of the SMN2 promoter–BLA reporter gene assay to HDAC inhibitors. Dose response experiments were completed in triplicate. Cells were incubated with varying concentrations of sodium butyrate and Trichostatin A (TSA) for 18 h prior to loading with the synthetic BLA substrate, CCF2/AM, and then BLA activity was measured. (**A**) Control SMN2 promoter assay NSC-34 cells. (**B**) SMN2 promoter assay cells treated with 2 mM sodium butyrate. (**C**) Sodium butyrate dose response experiment on the SMN2 promoter assay. $EC_{50} = 127$ μM and $EC_{100} = 2$ mM. (**D**) TSA dose response experiment on the SMN2 promoter assay, $EC_{50} = 17$ nM and $EC_{100} = 50$ nM. Error bars indicate standard deviation.

screening assay; a Z' value of 0.6 in 96 well format (described in Materials and Methods).

558 000 compound screening campaign of the SMN2 promoter assay

Approximately 558 000 unique compounds (695 410 total compounds) were screened against the SMN2 promoter assay. The screen was completed in two parts: (1) 115 954 compounds in high-throughput screening (HTS) mode using 384 well plates and (2) 579 456 (442 000 unique compounds) in ultra-high-throughput screening mode (UHTS) using 3456 well plates (52). During the screen, the majority of compound-treated wells displayed 460/530 nm fluorescence emission ratios comparable to those of the unstimulated cell controls, and only a small percentage of the total compounds screened possessed increased ratios, as shown in a representative plate

profile (Fig. 2). In order to mitigate the risk of missing potentially active compounds in the screen, we established a very liberal 'hit cutoff', where any compound possessing a 460/530 nm ratio greater than or equal to 67% of the mean BLA activity for the TSA-stimulated cells was chosen as a primary screening hit and underwent the retesting process. A total of 7275 primary screening hits was selected corresponding to a hit rate of 1.05%. These compounds were retested in duplicate using the original screening format. Of this set, 1030 compounds (14%) retested positive in at least a single well. To remove false positive compounds (those with endogenous 460 nm fluorescence), the 1030 compounds were incubated with the parental NSC-34 cell line, which lacks BLA, and 460 nm fluorescence was measured. This counter screen removed all but 137 compounds, and the remaining molecules were tested in 11-point dose response experiments performed in triplicate. Seventeen unique compounds, belonging to nine different structural scaffolds, designated A–I, displayed
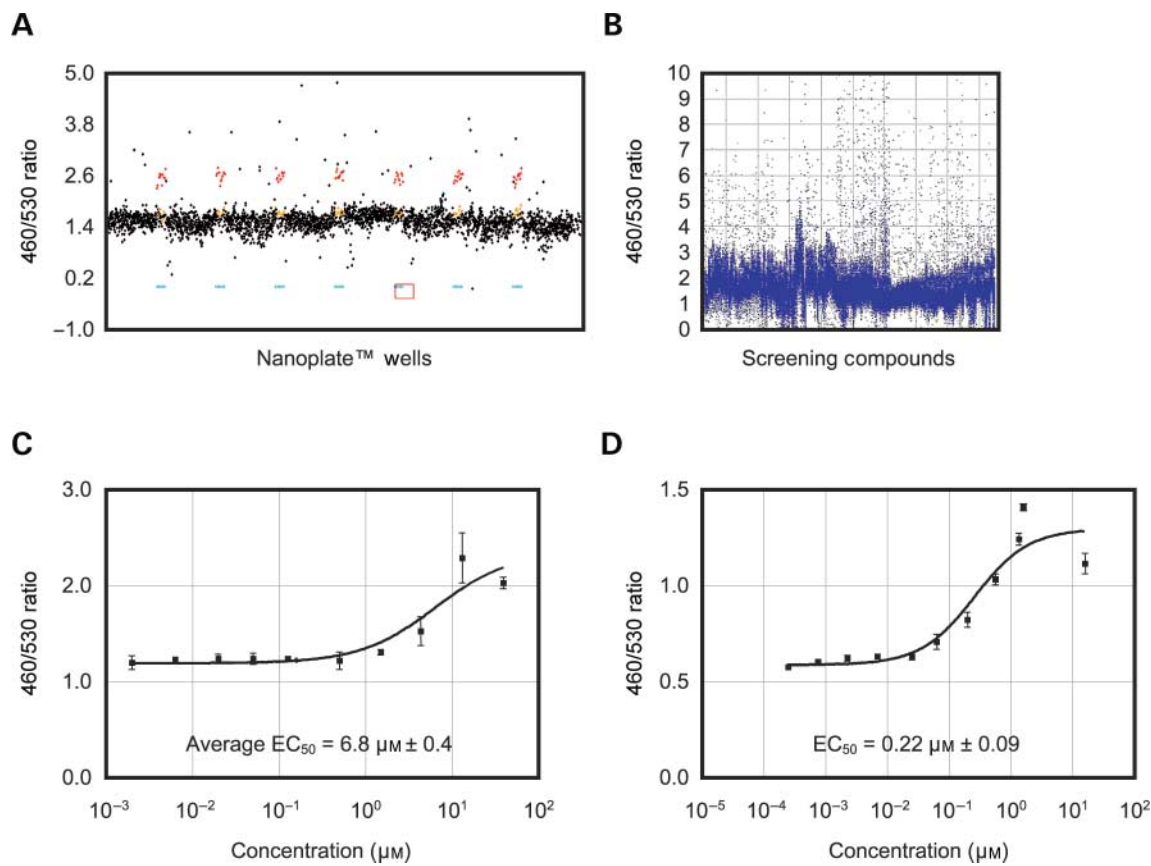
Figure 2. Compound screening against the SMN2 promoter assay. A total of 558 000 unique compounds were screened. The vast majority of the compounds (442 000) was screened in UHTS in 3456 Nanowell plates. (**A**) A representative Nanowell plate from the SMN2 promoter screen. Compound wells are shown in black, 100 nM TSA positive control wells are shown in red, untreated baseline control wells are shown in yellow and media only background control wells are shown in blue. (**B**) 460/530 nm ratios for the majority of compounds screened against the SMN2 promoter assay in UHTS format. Approximately 1% of compounds had a 460/530 nm ratio >67% of the mean ratio of TSA-treated cells and were scored as primary screening hits. (**C**) Dose response experiment on the promoter assay using Compound A. Dose response experiments using eleven concentration points were performed in triplicate with the highest concentration at 60 μM. Concentration decreased by one-third for each subsequent dose. Data for the 60 μM concentration point were not shown on the dose response curve because of decreased promoter activity caused by cellular toxicity. (**D**) Dose response experiment on the promoter assay using Compound G1 treatment. Dose response experiments using eleven concentration points were performed in triplicate with a high concentration of 12 μM. Concentration decreased by one-third for each subsequent data point.

sigmoidal dose response activity. Eight of the nine scaffolds have EC_{50} values in the single-digit micromolar range, whereas one compound class is significantly more potent with a sub-micromolar EC_{50} value (Table 1). These are within the typical potency range for screening hits (sub-micromolar potency compounds are considered very promising at this stage of drug development), and they are significantly more potent than current drug candidates for SMA, such as valproic acid and phenyl-butyrate, which have an EC_{50} in the millimolar range. Figure 2C and D shows dose response experiments on the promoter assay using two of the promising compounds A and G2, respectively. Compound A has an EC_{50} value of 6.8 ± 0.4 μM (Fig. 2C; a minimum of three independent dose response experiments were performed for each compound). Compound A begins to induce cellular toxicity in NC-34 cells between 30 and 40 μM, as measured in an XTT assay (Table 2). This results in an apparent declining response in promoter assay at the higher concentrations. The EC_{50} value for compound G2 is 0.22 ± 0.09 μM (Fig. 2D; a minimum of

Table 1. Summary of activity of the nine distinct chemical scaffolds identified in the SMN2 promoter screen

Scaffold	Number of distinct members	Average EC_{50} (μM)	BLA activity (fold induction)
A	1	7.0	2.0
B	1	7.0	1.3
C	4	3.0–10	2.0
D	1	9.0	>5.0
E	1	10.0	2.0
F	1	3.0	2.0
G	6	0.2–0.6	2.0
H	1	1.0	2.0
I	1	1.5	1.3

three independent dose response experiments were performed for each compound). The EC_{50} value for the other G scaffold compound presented in this paper, G1, is 0.33 ± 0.11 μM (data not shown).

Table 2. Summary of compound activities in the secondary assays

Compound name	Structural subtype	FL mRNA	Protein	Gems	Toxicity onset (μM)	Structure confirmed
A	Indole	Yes	Yes	Yes	30–40	Yes
D	Triazine	No	No	No	15–20	Yes
E	Unknown	Yes	No	ND	30–40	No
F	Phenyl-propylamine	Variable	No	No	>40	Yes
G1	Quinazoline	Yes	Yes	Yes	>40	Yes

Five compound types alter SMN mRNA transcript levels in SMA patient-derived cells

Six of the nine structural scaffolds (Scaffolds A–G) were deemed 'drug-like' due to their chemical properties (molecular mass, solubility, permeability, hydrogen bond donors and acceptors, reactive groups, etc.) and were advanced into secondary assay profiling. Compound efficacy in modulating endogenous SMN gene expression was determined by treating fibroblasts derived from two different Type 1 SMA patients and performing a previously described semi-quantitative RT–PCR assay that can detect four SMN splice forms—the full-length transcript (FL), one missing exon 7 (Δ7), one missing exon 5 (Δ5) and one missing both exons 7 and 5 (Δ5Δ7)—to assess human *SMN* transcript levels (53). The results obtained for each compound were highly consistent for the two SMA patient cell lines tested. All the compound classes except Scaffold B alter the endogenous SMN2 mRNA expression in both cell lines. Altered mRNA expression was observed in several different patterns among the five compound classes (Fig. 3A and B; also see Table 2 for a comparison of the effects on SMN mRNA among the five scaffolds).

The first mRNA pattern is exemplified by Compounds A, G1 and F, which shift SMN2 mRNA production primarily from the Δ7 to the full-length transcript. Two of these compounds, A and G1, are the most biologically promising and chemically attractive of the confirmed compound hits found in our screen (see Discussion) and underwent a more thorough analysis than the other three compound classes. Compounds A and G1 were tested at least four times with each cell type, and both highly consistently increased the relative abundance of the full-length transcript versus the Δ7 transcript in both SMA patient cell lines (representative examples shown in Fig. 3A and B). For example, after treatment with Compound A, the full-length/Δ7 *SMN* transcript ratio increased by 4.7 ± 1.4-fold in the 3813 cells (all RT–PCR errors are represented as SEM, Fig. 4D, $n = 4$, $P = 0.04$) and by 2.4 ± 0.3-fold for the 2806 cells (Fig. 4E, $n = 6$, $P < 0.001$). Similarly, Scaffold G1 increased the full-length/Δ7 transcript ratio by 2.5 ± 0.4-fold in the 3813 cells (Fig. 4D, $n = 4$, $P = 0.02$) and by 1.8 ± 0.1-fold in the 2806 cells (Fig. 4E, $n = 4$, $P < 0.004$). A similar result was observed with compound G2 (data not shown). Both compound classes consistently induced a greater change in the full-length/Δ7 *SMN* transcript ratio in 3813 cells than in 2806 cells. This pattern has been observed with several other compounds and may be due to the fact that the 3813 cells possess two copies of the human *SMN2* gene, whereas the

2806 cells have only a single copy (54). Compound F also alters the SMN mRNA pattern in the same manner by shifting SMN2 mRNA production from the Δ7 to the full-length transcript. Compound F treatment increased the full-length/Δ7 transcript ratio by an average of 2-fold (when all experiments completed in both cell lines were considered; $n = 5$). However, compound activity over the course of several months and multiple experiments were observed to be inconsistent in both cell lines. Only 60% of the experiments resulted in a positive response, with no apparent pattern or discernable cause for the varied results.

The second mRNA pattern induced by our compounds was observed with the use of Compound E, which increases total SMN2 mRNA levels without significantly altering the SMN2 full-length/Δ7 transcript ratio (Fig. 3A and B). This was the expected pattern for compounds isolated using a promoter activity assay. After Compound E treatment, the total amount of transcript produced from the SMN2 gene increased on average 1.82 ± 0.36-fold in the 2806 Type I patient-derived fibroblasts ($n = 3$, $P < 0.05$).

The third mRNA pattern is represented by Compound D, which increased the abundance of the rare Δ5Δ7 SMN2 transcript by 6.8 ± 2.4-fold in the 2806 Type I patient-derived fibroblasts ($n = 3$, $P < 0.05$; Fig. 3A and B). The mechanism responsible for the activity of Compound D was probed using a previously described SMN2 splicing assay that utilizes BLA activity to detect exon 7 inclusion in a human *SMN2* minigene containing exons 6 through 8 (55). In this assay, Compound D inhibited exon 7 inclusion at an IC_{50} value of $\sim$2 μM (10-fold lower than the EC_{50} value for cell toxicity). Compounds A and G1 did not show activity in the aforementioned splicing assay. We also tested the *in vitro* cytotoxicity of all five of these compounds using a colorimetric tetrazolium salt XTT assay in NSC-34 cells, which measures metabolic activity (56). Compound D showed the most significant toxicity with a cellular LD_{50} of $\sim$20 μM (Table 2).

Combination treatment with Compounds A and G enhance activity at the mRNA level in SMA patient fibroblasts

As the two lead compounds, A and G, may function by different mechanisms of action, they were tested in combination to see whether efficacy or potency improved. The first set of combination experiments utilized the SMN2 promoter assay. These experiments were designed as full dose response curves for each compound, in which a matrix of concentrations of both Compounds A and G were tested against
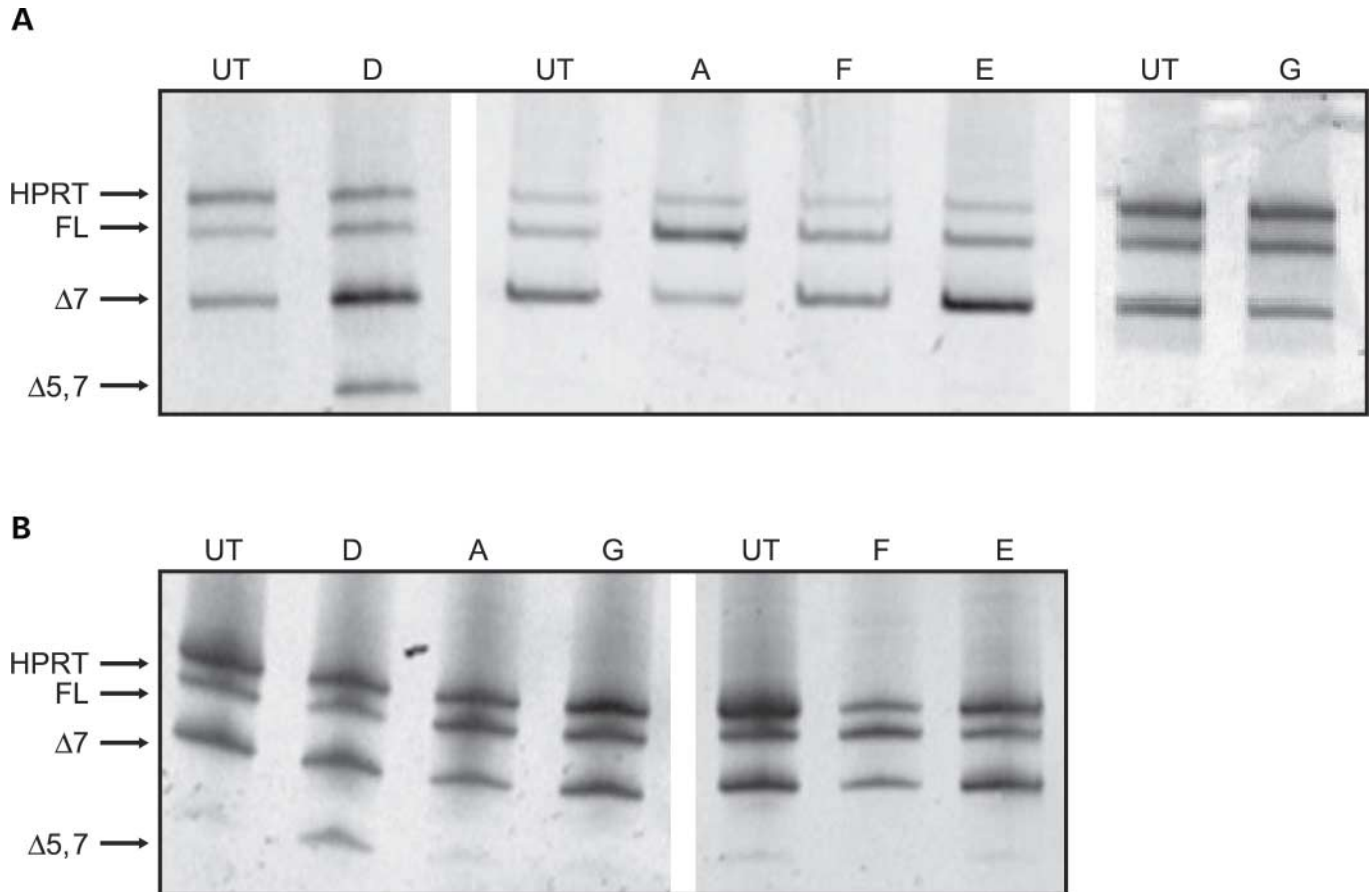
A

B

Figure 3. Effect of compound treatment on the SMN2 transcript in fibroblasts derived from Type 1 SMA patients. RT–PCR analysis was completed after a 24–48 h compound treatment in either 3813 (**A**) or 2806 (**B**) cells. All compounds were utilized at their EC_{100} concentrations as determined by dose response experiments performed on the SMN2 promoter assay. Compounds A, D and E were used at 12 μM. Compound F was used at 6 μM. Compound G1 was used at 5 μM. UT, untreated; HPRT, internal control gene used for the RT–PCR reaction; FL, full-length SMN transcript; Δ7, SMN transcript missing exon 7 and Δ5,7, SMN transcript missing exons 5 and 7.

one another. It was observed that treatment of the primary screening assay with Compounds A and G2 enhanced the level of BLA activity in a roughly additive fashion when compared with treatment with either compound alone, without any antagonistic effects of one compound on another (Fig. 4A). However, no reduction in potency for either compound was observed, and the EC_{100} concentrations of each compound required to obtain maximal stimulation of the SMN2 promoter assay were not reduced, suggesting that these two compounds possess different mechanisms of action in this assay. A similar level of synergy between Compounds A and G1 was also observed on promoter assay activation, using a narrower concentration range (data not shown).

The effect of Compounds A and G1 treatment on SMN mRNA levels was determined using RT–PCR analysis on the fibroblasts derived from the two different SMA patients. Because of the compound combination treatment results obtained in the promoter assay, EC_{100} compound concentrations were utilized. Combination treatment resulted in a dramatic increase in the full-length/Δ7 SMN transcript ratio in 3813 cells, significantly greater than the additive enhancement observed on the promoter assay (Fig 4). For example,

combination treatment in the 3813 cells increased the ratio by 43-fold when compared with a 4.7-fold increase for treatment with Compound A alone ($n = 3$, $P = 0.005$) and a 2.5-fold increase for treatment with Compound G1 alone ($n = 3$, $P = 0.004$). In the 2806 cells, combination treatment resulted in a 5.8-fold increase in the full-length/Δ7 transcript ratio when compared with only a 2.4-fold increase for Compound A treatment alone ($n = 5$, $P < 0.004$) and only 1.8-fold for Compound G alone ($n = 5$, $P < 0.006$). A similar result was observed with Compound G2 (data not shown). The synergistic influence of Compounds A and G on the relative abundance of the full-length/Δ7 transcripts level suggests that the two compounds may have different molecular mechanisms of action.

Compounds A and G increase total SMN protein levels and nuclear Gem/Cajal body numbers

We next tested whether the increase in full-length SMN2 RNA upon compound treatment resulted in an increase in SMN protein levels or in the number of SMN-containing nuclear gem/Cajal body structures, which are significantly reduced
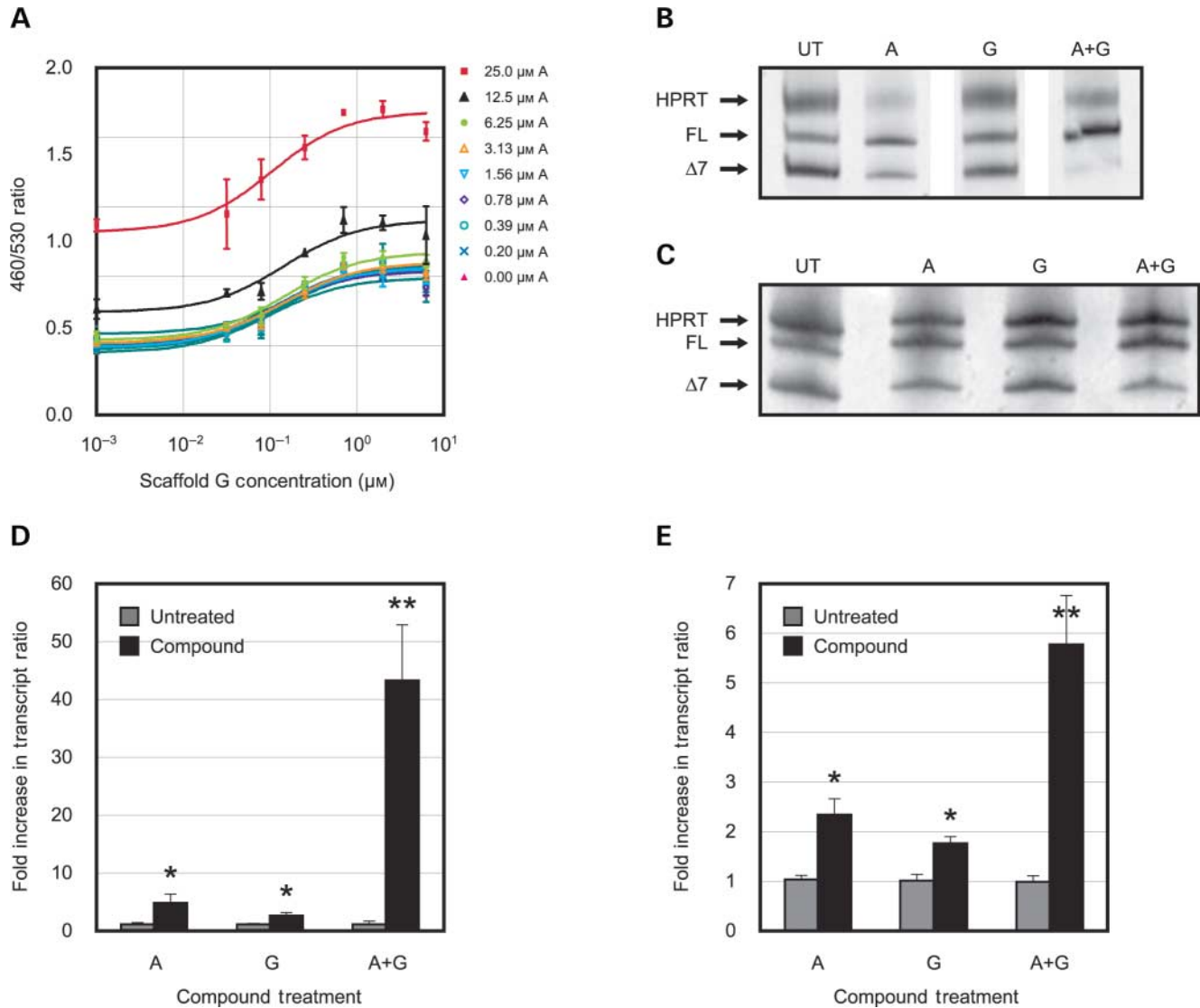
Figure 4. Combination treatment with both Compounds A and G1 enhances activity. (**A**) Representative dose response experiment with SMN2 promoter assay using Compounds A and G1. Each dosage point was performed in triplicate and cells treated for 18 h. The highest concentration of Compound A was 25 μM and decreased by 50% for each subsequent dosage point. The highest concentration of Compound G1 was 6.7 μM and decreased by one-third for each subsequent dosage point. (**B**) Representative RT–PCR analysis on 3813 cells treated with Compounds A and G1. Compounds were used at their EC_{100} concentrations (5 μM for Compound G1 and 12 μM for Compound A). (**C**) Representative RT–PCR analysis on 2806 cells treated with Compound A and G1. (**D**) Densitometric measurement of the full-length/Δ7 transcript ratio normalized to the ratio in unstimulated 3813 cells. Each value is a result of at least three independent experiments. $^{*}P \leq 0.04$ for A or G1 treatment alone compared to controls and $^{**}P \leq 0.005$ for A and G1 treatment compared to A or G1 treatment alone. (**E**) Densitometric measurement of the full-length/Δ7 transcript ratio normalized to the unstimulated ratio in 2806 cells. Each value is a result of at least five independent experiments. $^{*}P < 0.004$ for A or G1 treatment alone compared to controls. $^{**}P < 0.006$ for A and G1 treatment compared to A or G1 treatment alone. All error bars in the figure represent one standard error of the mean.

in cells from SMA patients (10,11,57). Total SMN protein levels were assessed in the 2806 cells with compounds A, D, E, F and G1 after 48 h of compound treatment. A 2–3-fold increase in SMN protein levels relative to α-tubulin and β-actin levels was consistently observed after treatment with Compounds A and G1 ($n = 4$, Fig. 5A). In contrast to the RT–PCR experiments measuring mRNA levels, A and G1 combination treatment did not consistently increase SMN protein levels relative to either compound alone (data not shown), which was surprising because a synergistic effect was observed between Compounds A and G on both the

promoter assay and the RT–PCR assay in two different cell lines. No significant effect on total SMN protein levels was observed with Compounds D, E or F (data not shown).

When compared with cells from either normal or non-symptomatic carrier individuals, fibroblasts derived from Type I SMA patients have few nuclear gems/Cajal bodies, the sub-nuclear compartments where SMN protein accumulates (10,11,57) (Fig. 5B). For example, 2806 cells have ~75% reduction in gem numbers when compared with cells derived from an SMA carrier (Fig. 5B). Treating 2806 cells with 12 μM of Compound A increased the gem/Cajal body
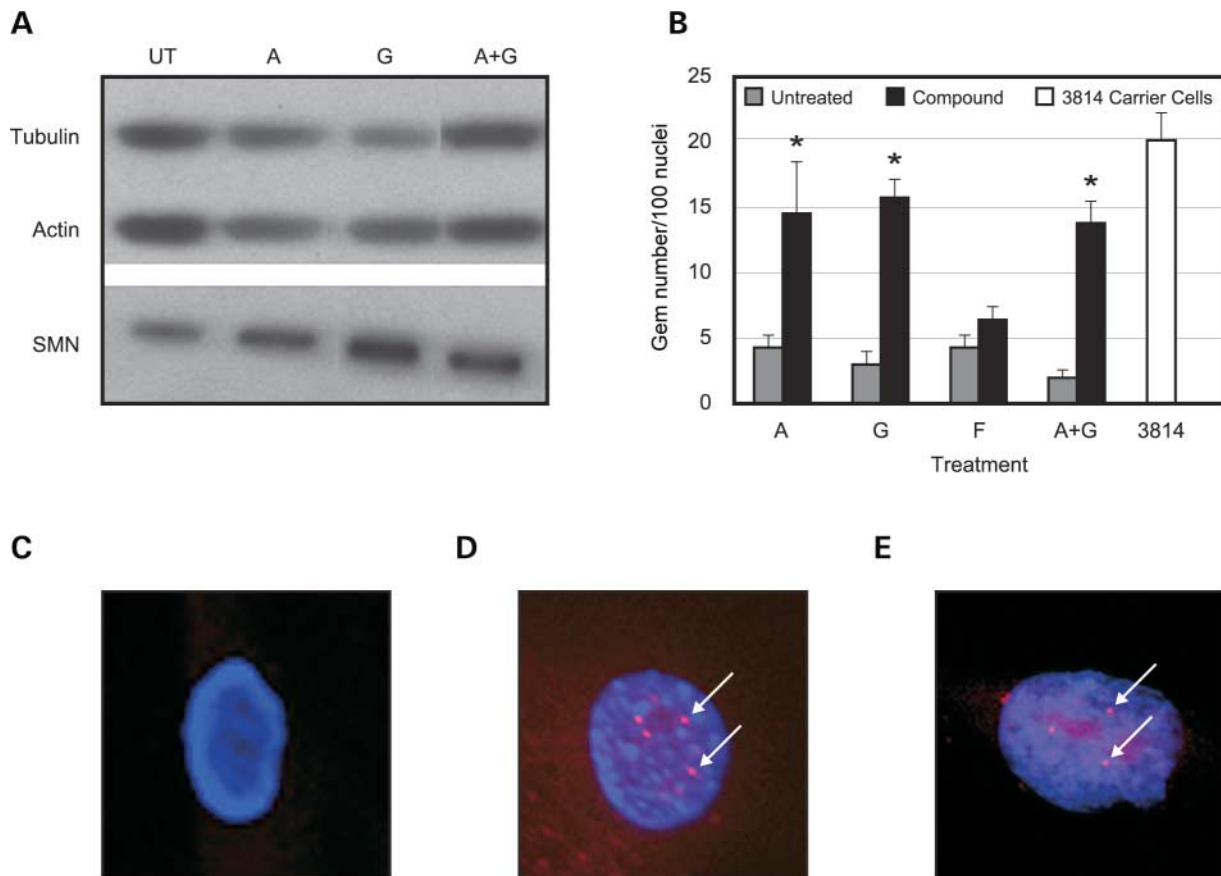
Figure 5. Compounds A and G1 increase SMN protein levels and gem/Cajal body numbers in fibroblasts derived from Type I SMA patients. (**A**) A representative western blot of SMN, β-actin and α-tubulin protein from 2806 SMA Type I fibroblasts. Cells were dosed daily with EC_{100} concentrations of compound for a total of 48 h. (**B**) Gem number in 2806 cells treated with Compounds A, G or F. 3814 cells are fibroblasts derived from an SMA carrier and thus provide a baseline for the number of gems found in a cell obtained from a non-symptomatic individual. 12 μM of Compound A was utilized and 5 μM of Compound G1. Error bars represent one standard error of the mean. *$P < 0.01$ when compared to DMSO controls. (**C**) Nuclei from untreated 2806 cells. (**D**) Nuclei from 2806 cells treated with Compound A for 5 days. (**E**) Nuclei from 2806 cells treated with Compound G1 for 5 days. Cells were stained with DAPI to identify nuclei (blue) and the SMN antibody (red) to identify gems/Cajal bodies (arrows).

count 3-fold to 14.5 ± 4-fold (error represented as SEM, $P < 0.01$). Treatment with 6.8 μM Compound A also increased the gem count by 3-fold to 13.08 ± 2.7-fold ($P = 0.006$). A 5 μM Compound G1 treatment increased the gem/Cajal body count 5-fold to 15.7 ± 1.4-fold in 2806 cells ($P = 0.002$), whereas no change in the number of gems was observed using a 10 μM Compound G1 treatment (3.63 ± 0.63). In 3813 cells, Compound G1 was effective in increasing the gem/Cajal body number at both compound concentrations (data not shown). Interestingly, Compound A did not increase the gem/Cajal body number in 3813 cells or the related 3814 carrier cells, perhaps indicating a tissue-specific mode of action for this compound (see Discussion). Combination A and G1 treatment in 2806 cells increased the gem/Cajal body number to 13.84 ± 1.63 ($P = 0.002$ when compared with DMSO treated cells), which is similar to the increase seen for cells treated with either Compound A or G1 individually. In the 3813 and 3814 cells, combination A and G1 treatment elicited a cellular response similar to that of Compound A treatment alone in this particular cell type—no increase in the gem/Cajal body number was

observed. Thus, as was predicted from the protein expression analysis, no synergistic effect was observed between compounds A and G1 in the gems assay. Moreover, Compound F did not increase the gem/Cajal body numbers in either cell line, which was expected as it does not increase SMN protein levels (serving as a negative control for this experiment). Considered together with the SMN transcript results, these data demonstrate that the compounds identified by their ability to increase reporter levels in the BLA promoter assay also act in SMA patient cells to increase the expression of endogenous SMN2 full-length transcript and protein levels and result in restoration of SMN nuclear localization to gems/Cajal bodies, suggesting that these compounds may be able to reverse the pathological phenotypes associated with loss of SMN function in SMA patients.

Examining the selectivity of action of Compounds A and G on the *SMN* gene promoter

As our HTS screening assay detects the activity of general transcriptional activators, such as HDAC inhibitors, in

addition to SMN-selective activators, it was essential to determine the extent of a compound's specificity to the SMN2 promoter. First, the ability of Compounds A and G to non-specifically activate transcription in NSC-34 cells was assessed. Clonal NSC-34 cell lines were generated in which a minimal thymidine kinase (tk) promoter drives BLA reporter gene expression. The chosen tk-BLA NSC-34 cell line possessed a very similar basal level of BLA activity as the SMN2 promoter assay and was responsive to TSA and sodium butyrate to a similar extent, indicating that this line is also capable of responding to HDAC inhibitors. Compounds A and four Scaffold G members (including G1 and G2) also increased the basal level of BLA activity in this cell line. The level of BLA induction by Compound A and its EC_{50} value in this assay were essentially identical to those elicited using the SMN2 promoter assay (Table 1). Several members of Scaffold G demonstrated more potent activity on the minimal tk-BLA NSC-34 assay, where the average EC_{50} value for the four members of Scaffold G was 90 nM when compared with an average of 300 nM on the promoter assay. The extent of BLA induction was identical in the two different NSC-34 cell assays for these two compound classes.

The aforementioned experiments suggested that compound types A and G act non-selectively to stimulate promoter activity in NSC-34 cells. To understand how broadly Compounds A and G stimulate gene expression, several BLA reporter cell lines representing various lineages and signaling pathways were examined: Hek/CRE (human embryonic kidney cells containing the BLA reporter under the control of a cAMP response element), SK-N-MC/CRE (human neuroblastoma cells possessing BLA under the control of a cAMP response element) and ME180/IRF [human cervical squamous carcinoma cells containing BLA under the control of interferon response factor element (58)]. These three 'CellSensor' lines were chosen because of their sensitivity of response to HDAC inhibitors. For example, 18 h stimulation with 2 mM sodium butyrate induced a clear increase in BLA activity in all three cell lines, in a range of 3–4.5-fold above baseline (Fig. 6A). In contrast, Compound A failed to induce activation of BLA activity in any of the three cell lines when tested up to a concentration of 36 μM (Fig. 6A).

When the SK-N-MC/CRE and Hek/CRE cell lines were tested with two structurally related members of the Scaffold G family (G1 and G2), significant BLA activation was not routinely observed. In roughly half of these experiments, the two Scaffold G family members tested induced BLA reporter activity modestly by 50–100%, with the potency of this induction significantly lower than their activity in the SMN2 promoter assay (observed EC_{50} values in these experiments were ~5–10 μM versus 200–300 nM in the SMN2 promoter assay, data for G1 shown in Fig. 6A). In addition, the degree of reporter activation by Scaffold G was much lower than either TSA or sodium butyrate in the CellSensor lines (data for G1 shown in Fig. 6A), whereas on the SMN2 promoter assay it was equivalent.

As the primary screening assay is responsive to HDAC inhibitors, the ability of Compounds A and G to inhibit HDAC activity was directly tested using an *in vitro* HDAC activity assay (BioMol). This assay utilizes a synthetic fluorescent substrate, which is deacetylated by HDACs (provided

in a HeLa cell extract). Dose response experiments performed with either Compound A or Compound G2 showed no inhibition of HDAC activity, in contrast to the TSA positive control (Fig. 6B and C). Experiments with Compound G1 utilized at 0.2 and 5 μM also did not inhibit HDAC activity in this assay (data not shown).

DISCUSSION

Using a cell-based reporter gene assay for small-molecule agonists of SMN2 transcription in a large-scale screening campaign, we have identified five distinct compound classes that reproducibly modulate SMN transcript levels in primary and secondary cellular assays (Fig. 7). Two of these classes, the indole compound (A) and the quinazoline compounds (G1, G2), increase the relative abundance of the full-length SMN transcript, increase SMN protein levels and increase gem/Cajal body numbers in SMA Type I patient-derived fibroblasts (Table 2). The quinazoline scaffold, which contains six members, is the most attractive, as it is the most potent compound class identified from our screen, it does not induce cellular toxicity at any of the tested concentrations, and its structure is amenable to chemical modification. Although the indole compound also shows promise, it has less attractive chemical properties; specifically, it contains a nitro group that is known to be susceptible to chemical modification *in vivo*. As there is no current therapy for SMA, we believe that both quinazoline and indole compound series warrant further investigation into their potential as SMA therapeutics through a medicinal chemistry effort which will generate structure-activity relationship data and improve potency and drug properties (e.g. bioavailability and pharmacokinetics). (A collaborative medicinal chemistry program is currently underway between deCODE Genetics and the Families of SMA.)

The other three compounds identified during screening, which only affect SMN expression at the mRNA level, are less attractive for several reasons. The triazine scaffold (D) displays cellular toxicity at the active concentration and promotes the production of the small undesirable SMN splice variants. The phenyl-propylamine molecule (F) increases the full-length SMN mRNA in an inconsistent manner, and it does not possess an attractive chemical structure for manipulation in a synthetic chemistry effort. The chemical structure of Compound E could not be verified through LC-mass spectrometry, and activity was lost when re-synthesized. However, after incubation in water overnight at 37°C, re-synthesized Compound E regains activity, suggesting that a breakdown product of Compound E is the active species (data not shown). Although the data on Compound E is not currently compelling, further experimentation could identify the active moiety.

At the onset of this project, it was not anticipated that the majority of the compounds would alter the SMN2 transcript ratio in addition to enhancing promoter activity. The initial expectation was that the identified compounds would enhance promoter activity, resulting in a coordinate increase in each SMN2 splice variant, similar to that observed with Compound E. However, four of the five compounds change
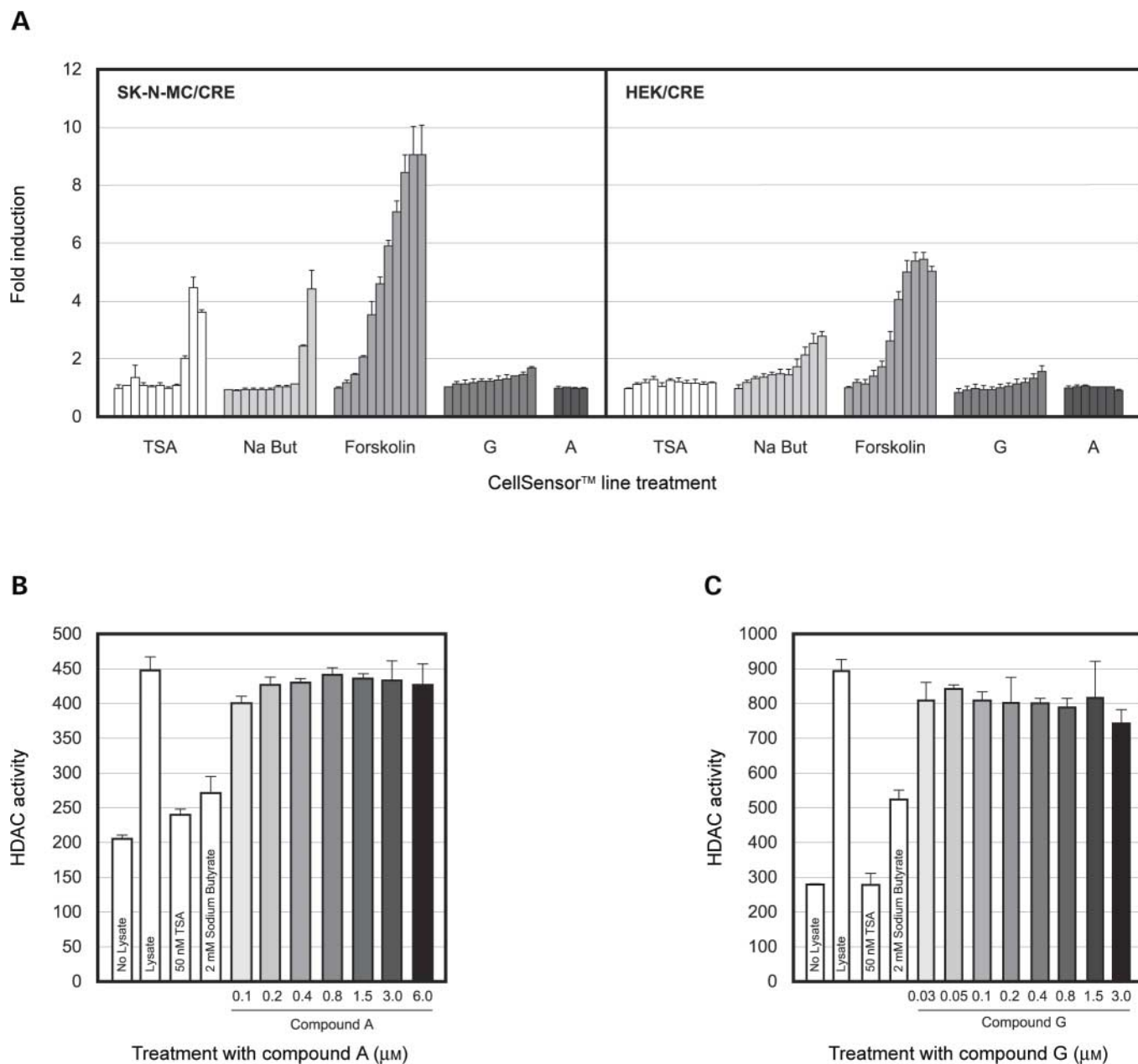
Figure 6. Testing of Compounds A and G using cell-based and *in vitro* assays for inhibition of HDAC activity. (**A**) Ability of compounds A and G1 to activate cell-based assays responsive to HDAC inhibitors. The SK-N-MC/CRE and the Hek/CRE CellSensor lines were tested with Trichostatin A (TSA), sodium butyrate (Na But) and Compounds A and G1. All dose response experiments were completed in triplicate. Dose response experiment started at a concentration of 167 nM for TSA and decreased by one-third for each subsequent dose. For Forskolin treatment, the dose response experiment began at 10 μM and decreased by one-third for each subsequent dose. For sodium butyrate treatment, experiments started at a concentration of 3.3 mM and decreased by one-third for each subsequent dose. Compound A was tested on the SK-N-MC cell line at 20, 12, 6 and 0 μM and tested on the Hek/CRE cell line starting at 36 μM and decreasing by one-third for each subsequent dose. Compound G1 was tested on both cell lines starting at 13 μM and decreasing by one-third with each subsequent dose. (**B** and **C**) Effect of Compounds A and G2 on an *in vitro* HDAC activity assay. The inhibitory HDAC activity of Compounds A and G2 was tested in dose response experiments in an HDAC activity assay from BioMol QunatiZyme, which utilizes a synthetic HDAC substrate that emits a fluorescent signal upon deacetylation in HeLa cell extracts. 50 nM TSA and 2 mM sodium butyrate were utilized as the positive controls. In Figure B, dose response experiments with Compound A were performed in triplicate at a high concentration of 6 μM, which decreased by 50% for each subsequent data point. In Figure C, dose response experiments with Compound G2 were performed in triplicate with a high concentration of 3 μM, which decreased by 50% for each subsequent data point.

the ratio of the full-length/Δ7 transcripts. Interestingly, during the course of our screening efforts, other research groups have identified compounds with similar characteristics. Each of these compounds—sodium butyrate (49), valproic acid (54,59)

and 4-phenylbutyrate (60)—function as HDAC inhibitors, which are known to activate transcription in ~2% of genes (47,48,61). The inhibition of HDACs enhances transcription through the hyperacetylation of histones, which alters the
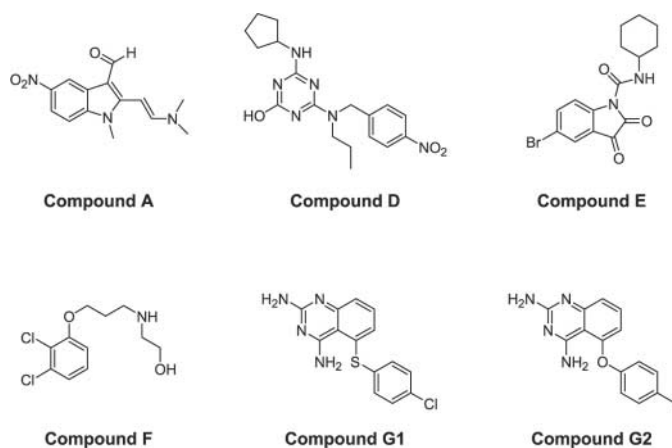
Figure 7. Structures of compounds tested for their ability to alter SMN2 mRNA expression levels or splicing patterns in fibroblasts derived from SMA patients. Compound A is an indole. Compound D is a triazine. The parental compound for scaffold E is an indole-dione compound. Compound F is a phenyl-propylamine compound. Compounds G1 and G2 are quinazoline.

chromatin architecture, allowing DNA to become accessible to the transcriptional machinery (61). The aforementioned HDAC inhibitors increase SMN levels in two different manners. First, they have a direct effect on SMN transcription and induce a 2–4-fold enhancement in SMN promoter activity. Secondly, these compounds alter the SMN2 splicing pattern, resulting in an increased full-length/$\Delta 7$ transcript ratio (49,54,59,60). Valproic acid and both forms of butyrate upregulate the expression of the *trans*-splicing factor Htra2-$\beta 1$, whose overexpression promotes exon 7 inclusion and can increase production of full-length SMN transcript (59).

Both the quinazoline and indole compounds uncovered in our screen possess characteristics similar to the HDAC inhibitors. For example, both compounds directly influence SMN2 promoter activity, as measured on the SMN2 promoter assay. Moreover, similar to the HDAC inhibitors, they shift the SMN2 splicing pattern to the production of the full-length transcript. The results on whether these compounds act as HDAC inhibitors are equivocal. Both compounds elicit non-selective gene activation in the NSC-34 cell line, but when tested on a broader range of promoters and cell types responsive to HDAC inhibitors, they did not cause significant transcriptional induction. Nor did the compounds show inhibitory activity in an *in vitro* HDAC assay. Interestingly, Compounds A, G1/G2 show synergy in activation of the promoter assay when used in combination with either valproic acid or sodium butyrate, both of which function as HDAC inhibitors (data not shown).

A possible explanation for this data is that our compounds function as HDAC inhibitors that inhibit only a subset of HDACs, some of which are expressed in a tissue-specific or a species-specific manner. To date, 18 human HDACs have been identified, which fall into three different classes (62–65). The class 1 deacetylases (1,2,3,8 and 11) are believed to be expressed in most tissues, whereas the class 2 deacetylases (4–7 and 9–10) display tissue-specific expression and are functionally regulated by nuclear/cytoplasmic shuffling, regulated by the activity of calcium/calmodulin-dependent

protein kinases [CaMKs; (66–68)]. The third class of human HDACs (SIRT1-7) is related to the yeast SIR2, an NAD+ dependent HDAC. Moreover, particular HDAC inhibitors have been shown to be specific to certain classes of deacetylases (69–70). Because the *in vitro* HDAC activity assay (BioMol QunatiZyme) we utilized has not definitively been shown to detect the activity of every HDAC, a more detailed examination of potential HDAC inhibitor activity of the present quinazoline and indole compounds is clearly warranted.

Several other interesting experimental observations arose from our studies of Compounds A and G. First, some aspects of compound efficacy are cell-line dependent. In both of the patient-derived cell lines, treatment with either Compound A or Compound G increased the ratio of full-length SMN transcript. However, Compound A resulted in increased protein and gem/Cajal body production in only one of the two cell lines (2806). Secondly, when used in combination, Compounds A and G displayed a synergistic influence on the amount of full-length SMN transcript produced. Synergy was not recapitulated when assessing protein levels or the numbers of gems/Cajal bodies present after combination treatment. Perhaps, this is due to deleterious effects of combination A and G treatment on nuclear transport of mRNA to the cytoplasm, on protein translation or on protein stability and degradation.

Can known small-molecule therapeutics be potential treatments for SMA?

Over the past several years, several small molecule compounds have been identified that increase SMN transcript and/or protein levels in SMA patient-derived cell lines. These include the short chain fatty acid butyrate and its derivative phenyl-butyrate (49,60), aclarubicin (55) and valproic acid (54,59). Although several of these molecules have been approved for use by the FDA for unrelated clinical indications, many possess major clinical liabilities when being considered for long-term use in children. For example, aclarubicin, a tetracycline derivative used as a chemotherapeutic, possesses very toxic side effects that make it inappropriate for long-term therapy (55). Moreover, butyrate has an extremely short half-life in human serum of less than 10 min, making it difficult to reach the millimolar plasma levels required for therapeutic benefit (71,72). The therapeutic use of the butyrate derivative, phenyl-butyrate, could be more promising. For example, phenyl-butyrate possesses an increased serum half-life of ~1 h (73), therapeutic concentrations of 2 mM have been previously attained in patients (74), it can penetrate the cerebrospinal fluid in primates (75), and it has been used previously in children to treat ornithine transcarbamylase deficiency (76). Recent human studies have shown that oral administration of phenyl-butyrate increased SMN expression in peripheral blood leukocytes in SMA patients and improved motor function (77,78). The third possibility for a small molecule therapeutic for SMA is valproic acid, which has been used as a long-term epilepsy therapy (79–82). However, it is known to increase the risk of hepatic toxicity in patients, which may be an even more significant issue in the pediatric

population. Currently, safety trials are underway in this population to assess this risk.

CONCLUSIONS

Our HTS screening was designed to identify transcriptional agonists for a compensatory gene for a recessive genetic disease and was enabled by the existence of a second copy of the SMN gene in humans (*SMN2*)—a unique genetic situation. We have described two validated leads using our unusual screening strategy. To date, the number of validated leads from cell-based 'black box' pathway screens is not numerous. A similar screening strategy has been described to discover small molecule activators of the utrophin gene for the treatment of Duchene's muscular dystrophy, but validated compounds have not yet been reported (83). Recently, indoprofen was identified in an HTS screen designed to detect molecules capable of correcting the *SMN2* gene-splicing pattern. This molecule seems to enhance SMN2 translation rather than alter the SMN2 mRNA splicing pattern (84,85). Small-molecule agonists of the hedgehog pathway have also been identified using a luciferase reporter gene assay (86), and several laboratories have successfully undertaken chemogenetic approaches using cell-based assays to identify compounds affecting different cellular processes (87–92).

The successful identification of compounds that increase SMN expression in our cell-based HTS screen provides corroboration that this is a useful drug discovery approach. A cell-based screening strategy is unbiased, not focusing on any particular molecular target that may or may not be well validated. One caveat of pathway screening is that the molecular targets remain unknown. While this is not a formal requirement for drug development, the delineation of the molecular target greatly facilitates advancement in the drug discovery process. Currently, the compounds found in this screen form the basis of a medicinal chemistry effort to produce new chemical entities with optimized drug-like properties such as potency and bioavailability. Once drug-like compounds have been synthesized, they will be tested for their ability to mitigate disease progression in SMA animal models.

MATERIALS AND METHODS

Cell culture

Human SMA Type I fibroblasts 2806 and 3813 were grown in DMEM containing 10% fetal calf serum, 2 mM glutamine and antibiotics. The mouse motor neuron cell line NSC-34 was grown in DMEM, 5% fetal bovine serum and antibiotics, including 500 µg/ml G418 (44).

Assay development

An *SMN2* promoter–BLA reporter gene vector was constructed as previously described (54). Briefly, a 3.4 kb *SMN2* promoter fragment was subcloned into the mammalian expression vector pCMVscript (45,46), replacing the CMV promoter in order to drive the expression of the BLA gene.

To generate the minimal-tk promoter–BLA construct, a DNA fragment containing the minimal-tk promoter was subcloned into a blunt ended *Eco*RI site and a *Hin*dIII site in the mammalian expression vector pCMVscript, replacing the CMV promoter. The *SMN2* promoter–BLA reporter gene construct and the minimal-tk promoter–BLA reporter gene construct were transfected into NSC-34 cells, using Lipofectamine reagent (Invitrogen). Pools of stably expressing cells were selected using 500 µg/ml G418 for 12 days, and single colonies were isolated by loading the stable pool with CCF2/AM, a fluorescent substrate of BLA, and sorting by flow cytometry BLA activity in the resulting clonal lines was measured as previously described (50,51). Briefly, after an 18 h incubation at 37°C, CCF2/AM, a fluorescent substrate of BLA, was added for 1 h at room temperature, and fluorescence emissions at 460 and 530 nm were then read in a fluorescence plate reader. The clonal cell lines were screened for low basal BLA activity and for increased BLA activity in response to HDAC inhibitors such as sodium butyrate or Trichostatin A (Sigma), which have been reported to regulate SMN promoter activity (49). The assay conditions were optimized in order to meet the assay validation of $Z' < 1$ ($Z' = 1 -$ [3(standard deviation of signal) + 3(standard deviation of the baseline)/signal–baseline] after stimulation with HDAC inhibitors in 96 well plate format (93).

Ultra-high-throughput screening

Approximately 442 000 unique compounds (580 000 total compounds) were screened on the SMN2 promoter assay using an UHTS format in 3456 well Nanoplates developed at Aurora Biosciences (52). Four days prior to screening, cells were plated at 50 000 cells/ml in a T225 flask. It was found that plating at a higher density and harvesting the cells < 72 h of culture time led to decreased responsiveness to HDAC inhibitors. On the day of screening, cells were manually removed from the flask, spun down and washed twice in DMEM without serum but with antibiotics. The cells were resuspended at 2 million cells/ml in DMEM. Cells were plated into Nanoplates within 1.5 h of harvesting to maintain viability. During this interval, cells were shaken periodically to prevent cell clumping. A robotic table-top reagent dispenser was utilized to dispense cells and other reagents into Nanoplates, which were pre-plated with 10 nl of compound dissolved in 75% DMSO. After reagent dispensation, the final volume of each well totaled 1.6 µl, resulting in a final compound concentration of 10 µM in 0.47% DMSO. Wells with test compound obtained two reagent dispensations: 0.4 µl of DMEM and 1.2 µl of cells, resulting in 2400 cells per well. Four types of control well were included 96 times on each plate. These included: (1) wells containing DMEM alone to determine background levels of fluorescence; (2) wells containing DMEM, DMSO and 2400 cells to give the baseline level of BLA activity; (3) wells containing DMEM, DMSO, 2400 cells and 75 nM TSA and (4) wells containing DMEM, DMSO, 2400 cells and 100 nM TSA to indicate stimulated levels of BLA activity. After an 18 h incubation at 37°C, 0.4 µl CCF4/AM, a fluorescent substrate of BLA was added to each well, plates were incubated at room temperature for 2 h, and fluorescence emissions at 460

and 530 nm were read using a Nanoplate reader (NPR). Prior to selecting primary screening hits, each individual plate underwent a round of quality control analysis. This included determination of both the Z' factor described previously and the dynamic range between the 96 untreated wells and the 96 wells treated with 100 nM TSA on each plate. Those compound plates that did not pass quality control were re-screened and not used for hit selection (84% of the 197 total plates passed quality control analysis). The average Z' value for UHTS screening was 1.0 ± 0.2 and the dynamic range was 1.5 ± 0.1.

High-throughput screening

115 954 unique compounds were screened in HTS mode in 384 well plates. Cells were grown and harvested identically to those used in the UHTS portion of the screen. 17 500 cells per well were used in a final volume of 90 µl. The final compound concentration was 10 µM and the final concentration of DMSO per well was 0.375%. A control reference plate was run for every 10 compound screening plates. Fifty nanomolar TSA was used as the positive control. When the reference plate failed to pass the quality control analysis described previously, the 10 associated compound plates were re-screened.

Primary screening hit selection

Each compound possessing 460/530 nm ratios with 67% of the mean BLA activity level in the TSA-stimulated cells on its own screening plate was chosen as a potential primary screening hit. Prior to final hit selection, compound wells with very low green fluorescence (530 nm reading) were excluded, as this typically indicates cell death, which artificially increases the 460/530 nm ratio. Primary screening hits were re-tested in duplicate using the original screening format (either in 384 well or 3456 well plates).

Dose response experiments

Twelve point dose response experiments were performed in triplicate on the SMN2 promoter assay in 96 well plates. Each well contained 50 000 cells in a volume of 100 µl. The highest compound concentration tested was 40 µM, which was decreased by one-third with each subsequent dose. Cells were harvested as described previously and plated at the time of compound addition. After an 18 h compound treatment, BLA activity was measured as previously described. Dose response curves were fitted and EC50 values were determined using the computer program Prism (GraphPad).

XTT assay

Compound toxicity was measured using a XTT cell proliferation assay (Roche), which measures mitochondrial function. Cell proliferation after compound treatment for 24–72 h was determined in 96 well plates using the dose response experiments described previously. The highest compound concentration in these experiments was typically 40 µM. The XTT

assay was then run according to the manufacturer's specifications.

Semi-quantitative RTPCR analysis of the SMN transcripts

3813 and 2806 fibroblasts derived from Type I SMA patients were treated for 24–48 h with compounds. All compounds were utilized at their EC_{100} concentrations as determined by dose response experiments performed on the SMN2 promoter assay. Compounds A, D and E were used at 12 µM, Compound F was used at 6 µM and Compound G was used at 5 µM. Cells were plated 24 h prior to treatment. Media were changed daily and fresh compound added. Total RNA was isolated from untreated and treated cells, using the RNAeasy Kit (Qiagen), as described by the manufacturer's recommendations. First strand cDNA synthesis was performed with 2 µg of total RNA using an oligo d (T) primer. To amplify endogenous SMN RNA, a multiplex RT–PCR was performed as described in (53). The following SMN primers were utilized: 541C380 (5′-GTGAGAA CTCCAGGTCTCCTGG-3′) and 541C1120 (5′-CTACAACACCCTTCTCACAG-3′). These primers amplify exons 4 to 8 of the SMN gene, yielding four possible RT–PCR products (full-length SMN transcript and three isoforms lacking exon 5 and/or 7). Amplification of the hypoxanthine guanine phosphoribosyltransferase gene (HPRT) was performed in a multiplex format as a loading control for the amount of mRNA utilized in the reaction. The following primers specific to the HPRT gene were used: HPRT-forward (5′-TGTAATGACCAGTCAACAGG-3′) and HPRT-reverse (5′-AATGACTGCTTCTTACTTTTCT-3′). The cycling conditions were as follows: 95°C for 5 min, 25 cycles of 1 min at 95°C, 2 min at 55°C, 3 min at 72°C and a final extension time of 8 min at 72°C. The resulting PCR products were electrophoresed on a 6% polyacrylimide TBE–urea gel, stained for 20 min with Vistra Green nuclei acid stain (Pharmacia) and the intensity of individual bands quantified on a Storm Phosphoimager using the blue fluorescent detector at a PMT value between 650 and 800. Full-length/$\Delta 7$ SMN transcript ratios were determined from at least one of two patient-derived fibroblast cell lines in a minimum of three independent experiments. Differences in ratios after treatments were determined to be significant by an independent two-tailed t-test, with $P < 0.05$. Compounds A and G underwent more rigorous analysis with testing at least four independent times in both cell lines. In 2806 cells, six independent Compound A treatments were completed, four with Compound G and five with combination A and G. In 3813 cells, four independent treatments were completed for Compound A, four with Compound G and three with combination A and G.

Western blot analysis

2806 Type 1 SMA fibroblasts cells were plated at 50 000 to 100 000 cells per 10 cm dish and treated with compound for 48 h. Compound A and G treatments were performed four independent times. Media and compound were changed daily. Cells were harvested at 50–60% confluence. The cells were harvested with trypsin, washed two times with PBS

and collected by centrifugation. The resultant cell pellet was re-suspended in 45 µl of RIPA buffer plus protease inhibitors and lysed on ice for 30 min. Then, 45 µl of NuPAGE LDS sample buffer was added to the sample. An aliquot of 1 µl of reducing agent was then added to 10 µl of each sample and then boiled for 10 min. An aliquot of 5–10 µl of protein sample was separated on a NuPAGE 10% Bis–Tris gel in 1× NuPAGE MOPS running buffer. The protein was transferred to a PVDF membrane and blocked for 1 h at room temperature with TBS containing 5% milk and 0.1% Tween. Each blot was cut in half and the SMN and loading control portions processed separately. Primary antibodies specific to SMN (Transduction Labs) were incubated for 16 h at 4°C, whereas loading control antibodies (either anti-actin and/or anti-β-tubulin from Sigma) were incubated for 1 h at room temperature. Membranes were then incubated for 1 h with an HRP-linked anti-mouse IgG secondary antibody, detected with chemiluminescence using the ECL Plus kit (Amersham) and exposed to film.

Immunocytochemistry and Gem/Cajal body analysis

Immunofluorescence staining on 3813 and 2806 Type 1 SMA patient-derived fibroblasts was performed as described previously. Cells were seeded into dishes containing three coverslips (1 cm^2) at a density of 100 cells/cm^2 and stained with the MANSMA2 anti-SMN antibody, diluted 1:100 (55). Gem counting was done using a Nikon microscope equipped with a dual band pass DAPI/TRITC filter, and images were captured with a Magnafire digital camera (Optronics). Gems were counted and expressed as number per 100 nuclei. Statistical analysis comparing gem number of untreated cells to each treatment dose was done using an independent two-sided *t*-test. Each compound was treated at two doses, including 12 and 6.8 µM for Compound A and 5 and 10 µM for Compound G.

Compounds

Compounds A, F and E are commercially available from ChemBridge. Compounds G1 and G2 can be obtained from Maybridge.

REFERENCES

1. Roberts, D.F., Chavez, J. and Court, S.D. (1970) The genetic component in child mortality. *Arch. Dis. Child.*, **45**, 33–38.
2. Feldkotter, M., Schwarzer, V., Wirth, R., Wienker, T.F. and Wirth, B. (2002) Quantitative analyses of SMN1 and SMN2 based on real-time lightCycler PCR: fast and highly reliable carrier testing and prediction of severity of spinal muscular atrophy. *Am. J. Hum. Genet.*, **70**, 358–368.
3. Pearn, J. (1978) Incidence, prevalence, and gene frequency studies of chronic childhood spinal muscular atrophy. *J. Med. Genet.*, **15**, 409–413.
4. McAndrew, P.E., Parsons, D.W., Simard, L.R., Rochette, C., Ray, P.N., Mendell, J.R., Prior, T.W. and Burghes, A.H. (1997) Identification of proximal spinal muscular atrophy carriers and patients by analysis of SMNT and SMNC gene copy number. *Am. J. Hum. Genet.*, **60**, 1411–1422.
5. Lefebvre, S., Burglen, L., Reboullet, S., Clermont, O., Burlet, P., Viollet, L., Benichou, B., Cruaud, C., Millasseau, P., Zeviani, M. *et al.* (1995) Identification and characterization of a spinal muscular atrophy-determining gene. *Cell*, **80**, 155–165.
6. Lorson, C.L., Hahnen, E., Androphy, E.J. and Wirth, B. (1999) A single nucleotide in the SMN gene regulates splicing and is responsible for spinal muscular atrophy. *Proc. Natl Acad. Sci. USA*, **96**, 6307–6311.
7. Monani, U.R., Lorson, C.L., Parsons, D.W., Prior, T.W., Androphy, E.J., Burghes, A.H. and McPherson, J.D. (1999) A single nucleotide difference that alters splicing patterns distinguishes the SMA gene SMN1 from the copy gene SMN2. *Hum. Mol. Genet.*, **8**, 1177–1183.
8. Lorson, C.L., Strasswimmer, J., Yao, J.M., Baleja, J.D., Hahnen, E., Wirth, B., Le, T., Burghes, A.H. and Androphy, E.J. (1998) SMN oligomerization defect correlates with spinal muscular atrophy severity. *Nat. Genet.*, **19**, 63–66.
9. Young, P.J., Man, N.T., Lorson, C.L., Le, T.T., Androphy, E.J., Burghes, A.H. and Morris, G.E. (2000) The exon 2b region of the spinal muscular atrophy protein, SMN, is involved in self-association and SIP1 binding. *Hum. Mol. Genet.*, **9**, 2869–2877.
10. Coovert, D.D., Le, T.T., McAndrew, P.E., Strasswimmer, J., Crawford, T.O., Mendell, J.R., Coulson, S.E., Androphy, E.J., Prior, T.W. and Burghes, A.H. (1997) The survival motor neuron protein in spinal muscular atrophy. *Hum. Mol. Genet.*, **6**, 1205–1214.
11. Lefebvre, S., Burlet, P., Liu, Q., Bertrandy, S., Clermont, O., Munnich, A., Dreyfuss, G. and Melki, J. (1997) Correlation between severity and SMN protein level in spinal muscular atrophy. *Nat. Genet.*, **16**, 265–269.
12. Lorson, C.L. and Androphy, E.J. (2000) An exonic enhancer is required for inclusion of an essential exon in the SMA-determining gene SMN. *Hum. Mol. Genet.*, **9**, 259–265.
13. Kashima, T. and Manley, J.L. (2003) A negative element in SMN2 exon 7 inhibits splicing in spinal muscular atrophy. *Nat. Genet.*, **34**, 460–463.
14. Cartegni, L. and Krainer, A.R. (2002) Disruption of an SF2/ASF-dependent exonic splicing enhancer in SMN2 causes spinal muscular atrophy in the absence of SMN1. *Nat. Genet.*, **30**, 377–384.
15. Hofmann, Y. and Wirth, B. (2002) hnRNP-G promotes exon 7 inclusion of survival motor neuron (SMN) via direct interaction with Htra2-beta1. *Hum. Mol. Genet.*, **11**, 2037–2049.
16. Young, P.J., DiDonato, C.J., Hu, D., Kothary, R., Androphy, E.J. and Lorson, C.L. (2002) SRp30c-dependent stimulation of survival motor neuron (SMN) exon 7 inclusion is facilitated by a direct interaction with hTra2 beta 1. *Hum. Mol. Genet.*, **11**, 577–587.
17. Liu, Q. and Dreyfuss, G. (1996) A novel nuclear structure containing the survival of motor neurons protein. *EMBO J.*, **15**, 3555–3565.
18. Young, P.J., Le, T.T., thi Man, N., Burghes, A.H. and Morris, G.E. (2000) The relationship between SMN, the spinal muscular atrophy protein, and nuclear coiled bodies in differentiated tissues and cultured cells. *Exp. Cell Res.*, **256**, 365–374.
19. Yong, J., Wan, L. and Dreyfuss, G. (2004) Why do cells need an assembly machine for RNA-protein complexes? *Trends Cell Biol.*, **14**, 226–232.
20. Gubitz, A.K., Feng, W. and Dreyfuss, G. (2004) The SMN complex. *Exp. Cell Res.*, **296**, 51–56.
21. Terns, M.P. and Terns, R.M. (2001) Macromolecular complexes: SMN—the master assembler. *Curr. Biol.*, **11**, R862–R864.
22. Meister, G., Hannus, S., Plottner, O., Baars, T., Hartmann, E., Fakan, S., Laggerbauer, B. and Fischer, U. (2001) SMNrp is an essential pre-mRNA splicing factor required for the formation of the mature spliceosome. *EMBO J.*, **20**, 2304–2314.

23. Pellizzoni, L., Kataoka, N., Charroux, B. and Dreyfuss, G. (1998) A novel function for SMN, the spinal muscular atrophy disease gene product, in pre-mRNA splicing. *Cell*, **95**, 615–624.

24. Strasswimmer, J., Lorson, C.L., Breiding, D.E., Chen, J.J., Le, T., Burghes, A.H. and Androphy, E.J. (1999) Identification of survival motor neuron as a transcriptional activator-binding protein. *Hum. Mol. Genet.*, **8**, 1219–1226.

25. Williams, B.Y., Hamilton, S.L. and Sarkar, H.K. (2000) The survival motor neuron protein interacts with the transactivator FUSE binding protein from human fetal brain. *FEBS Lett.*, **470**, 207–210.

26. Lefebvre, S., Burlet, P., Viollet, L., Bertrandy, S., Huber, C., Belser, C. and Munnich, A. (2002) A novel association of the SMN protein with two major non-ribosomal nucleolar proteins and its implication in spinal muscular atrophy. *Hum. Mol. Genet.*, **11**, 1017–1027.

27. Wehner, K.A., Ayala, L., Kim, Y., Young, P.J., Hosler, B.A., Lorson, C.L., Baserga, S.J. and Francis, J.W. (2002) Survival motor neuron protein in the nucleolus of mammalian neurons. *Brain Res.*, **945**, 160–173.

28. Young, P.J., Day, P.M., Zhou, J., Androphy, E.J., Morris, G.E. and Lorson, C.L. (2002) A direct interaction between the survival motor neuron protein and p53 and its relationship to spinal muscular atrophy. *J. Biol. Chem.*, **277**, 2852–2859.

29. Vyas, S., Bechade, C., Riveau, B., Downward, J. and Triller, A. (2002) Involvement of survival motor neuron (SMN) protein in cell death. *Hum. Mol. Genet.*, **11**, 2751–2764.

30. Kerr, D.A., Nery, J.P., Traystman, R.J., Chau, B.N. and Hardwick, J.M. (2000) Survival motor neuron protein modulates neuron-specific apoptosis. *Proc. Natl Acad. Sci. USA*, **97**, 13312–13317.

31. Rossoll, W., Kroning, A.K., Ohndorf, U.M., Steegborn, C., Jablonka, S. and Sendtner, M. (2002) Specific interaction of Smn, the spinal muscular atrophy determining gene product, with hnRNP-R and gry-rbp/hnRNP-Q: a role for Smn in RNA processing in motor axons? *Hum. Mol. Genet.*, **11**, 93–105.

32. Rossoll, W., Jablonka, S., Andreassi, C., Kroning, A.K., Karle, K., Monani, U.R. and Sendtner, M. (2003) Smn, the spinal muscular atrophy-determining gene product, modulates axon growth and localization of beta-actin mRNA in growth cones of motoneurons. *J. Cell Biol.*, **163**, 801–812.

33. Zhang, H.L., Pan, F., Hong, D., Shenoy, S.M., Singer, R.H. and Bassell, G.J. (2003) Active transport of the survival motor neuron protein and the role of exon-7 in cytoplasmic localization. *J. Neurosci.*, **23**, 6627–6637.

34. Fan, L. and Simard, L.R. (2002) Survival motor neuron (SMN) protein: role in neurite outgrowth and neuromuscular maturation during neuronal differentiation and development. *Hum. Mol. Genet.*, **11**, 1605–1614.

35. McWhorter, M.L., Monani, U.R., Burghes, A.H. and Beattie, C.E. (2003) Knockdown of the survival motor neuron (Smn) protein in zebrafish causes defects in motor axon outgrowth and pathfinding. *J. Cell Biol.*, **162**, 919–931.

36. Vitali, T., Sossi, V., Tiziano, F., Zappata, S., Giuli, A., Paravatou-Petsotas, M., Neri, G. and Brahe, C. (1999) Detection of the survival motor neuron (SMN) genes by FISH: further evidence for a role for SMN2 in the modulation of disease severity in SMA patients. *Hum. Mol. Genet.*, **8**, 2525–2532.

37. Mazzei, R., Gambardella, A., Conforti, F.L., Magariello, A., Patitucci, A., Gabriele, A.L., Sprovieri, T., Labate, A., Valentino, P., Bono, F. et al. (2004) Gene conversion events in adult-onset spinal muscular atrophy. *Acta Neurol. Scand.*, **109**, 151–154.

38. Campbell, L., Potter, A., Ignatius, J., Dubowitz, V. and Davies, K. (1997) Genomic variation and gene conversion in spinal muscular atrophy: implications for disease process and clinical phenotype. *Am. J. Hum. Genet.*, **61**, 40–50.

39. Cifuentes-Diaz, C., Frugier, T., Tiziano, F.D., Lacene, E., Roblot, N., Joshi, V., Moreau, M.H. and Melki, J. (2001) Deletion of murine SMN exon 7 directed to skeletal muscle leads to severe muscular dystrophy. *J. Cell Biol.*, **152**, 1107–1114.

40. Frugier, T., Tiziano, F.D., Cifuentes-Diaz, C., Miniou, P., Roblot, N., Dierich, A., Le Meur, M. and Melki, J. (2000) Nuclear targeting defect of SMN lacking the C-terminus in a mouse model of spinal muscular atrophy. *Hum. Mol. Genet.*, **9**, 849–858.

41. Hsieh-Li, H.M., Chang, J.G., Jong, Y.J., Wu, M.H., Wang, N.M., Tsai, C.H. and Li, H. (2000) A mouse model for spinal muscular atrophy. *Nat. Genet.*, **24**, 66–70.

42. Monani, U.R., Coovert, D.D. and Burghes, A.H. (2000) Animal models of spinal muscular atrophy. *Hum. Mol. Genet.*, **9**, 2451–2457.

43. Monani, U.R., Pastore, M.T., Gavrilina, T.O., Jablonka, S., Le, T.T., Andreassi, C., DiCocco, J.M., Lorson, C., Androphy, E.J., Sendtner, M. et al. (2003) A transgene carrying an A2G missense mutation in the SMN gene modulates phenotypic severity in mice with severe (type I) spinal muscular atrophy. *J. Cell Biol.*, **160**, 41–52.

44. Cashman, N.R., Durham, H.D., Blusztajn, J.K., Oda, K., Tabira, T., Shaw, I.T., Dahrouge, S. and Antel, J.P. (1992) Neuroblastoma x spinal cord (NSC) hybrid cell lines resemble developing motor neurons. *Dev. Dyn.*, **194**, 209–221.

45. Echaniz-Laguna, A., Miniou, P., Bartholdi, D. and Melki, J. (1999) The promoters of the survival motor neuron gene (SMN) and its copy (SMNc) share common regulatory elements. *Am. J. Hum. Genet.*, **64**, 1365–1370.

46. Monani, U.R., McPherson, J.D. and Burghes, A.H. (1999) Promoter analysis of the human centromeric and telomeric survival motor neuron genes (SMNC and SMNT). *Biochim. Biophys. Acta*, **1445**, 330–336.

47. Kelly, W.K., O'Connor, O.A. and Marks, P.A. (2002) Histone deacetylase inhibitors: from target to clinical trials. *Expert Opin. Investig. Drugs*, **11**, 1695–1713.

48. Van Lint, C., Emiliani, S. and Verdin, E. (1996) The expression of a small fraction of cellular genes is changed in response to histone hyperacetylation. *Gene Expr.*, **5**, 245–253.

49. Chang, J.G., Hsieh-Li, H.M., Jong, Y.J., Wang, N.M., Tsai, C.H. and Li, H. (2001) Treatment of spinal muscular atrophy by sodium butyrate. *Proc. Natl Acad. Sci. USA*, **98**, 9808–9813.

50. Zlokarnik, G. (2000) Fusions to beta-lactamase as a reporter for gene expression in live mammalian cells. *Methods Enzymol.*, **326**, 221–244.

51. Zlokarnik, G., Negulescu, P.A., Knapp, T.E., Mere, L., Burres, N., Feng, L., Whitney, M., Roemer, K. and Tsien, R.Y. (1998) Quantitation of transcription and clonal selection of single living cells with beta-lactamase as reporter. *Science*, **279**, 84–88.

52. Mere, L., Bennett, T., Coassin, P., England, P., Hamman, B., Rink, T., Zimmerman, S. and Negulescu, P. (1999) Miniaturized FRET assays and microfluidics: key components for ultra-high-throughput screening. *Drug Discov. Today*, **4**, 363–369.

53. Parsons, D.W., McAndrew, P.E., Iannaccone, S.T., Mendell, J.R., Burghes, A.H. and Prior, T.W. (1998) Intragenic telSMN mutations: frequency, distribution, evidence of a founder effect, and modification of the spinal muscular atrophy phenotype by cenSMN copy number. *Am. J. Hum. Genet.*, **63**, 1712–1723.

54. Sumner, C.J., Huynh, T.N., Markowitz, J.A., Perhac, J.S., Hill, B., Coovert, D.D., Schussler, K., Chen, X., Jarecki, J., Burghes, A.H. et al. (2003) Valproic acid increases SMN levels in spinal muscular atrophy patient cells. *Ann. Neurol.*, **54**, 647–654.

55. Andreassi, C., Jarecki, J., Zhou, J., Coovert, D.D., Monani, U.R., Chen, X., Whitney, M., Pollok, B., Zhang, M., Androphy, E. et al. (2001) Aclarubicin treatment restores SMN levels to cells derived from type I spinal muscular atrophy patients. *Hum. Mol. Genet.*, **10**, 2841–2849.

56. Mosmann, T. (1983) Rapid colorimetric assay for cellular growth and survival: application to proliferation and cytotoxicity assays. *J. Immunol. Methods*, **65**, 55–63.

57. Patrizi, A.L., Tiziano, F., Zappata, S., Donati, M.A., Neri, G. and Brahe, C. (1999) SMN protein analysis in fibroblast, amniocyte and CVS cultures from spinal muscular atrophy patients and its relevance for diagnosis. *Eur. J. Hum. Genet.*, **7**, 301–309.

58. Durick, K. and Negulescu, P. (2001) Cellular biosensors for drug discovery. *Biosens. Bioelectron.*, **16**, 587–592.

59. Brichta, L., Hofmann, Y., Hahnen, E., Siebzehnrubl, F.A., Raschke, H., Blumcke, I., Eyupoglu, I.Y. and Wirth, B. (2003) Valproic acid increases the SMN2 protein level: a well-known drug as a potential therapy for spinal muscular atrophy. *Hum. Mol. Genet.*, **12**, 2481–2489.

60. Andreassi, C., Angelozzi, C., Tiziano, F.D., Vitali, T., De Vincenzi, E., Boninsegna, A., Villanova, M., Bertini, E., Pini, A., Neri, G. et al. (2004) Phenylbutyrate increases SMN expression *in vitro*: relevance for treatment of spinal muscular atrophy. *Eur. J. Hum. Genet.*, **12**, 59–65.

61. Pazin, M.J. and Kadonaga, J.T. (1997) What's up and down with histone deacetylation and transcription? *Cell*, **89**, 325–328.

62. Khochbin, S., Verdel, A., Lemercier, C. and Seigneurin-Berny, D. (2001) Functional significance of histone deacetylase diversity. *Curr. Opin. Genet. Dev.*, **11**, 162–166.

63. Gray, S.G. and Ekstrom, T.J. (2001) The human histone deacetylase family. *Exp. Cell Res.*, **262**, 75–83.

64. de Ruijter, A.J., van Gennip, A.H., Caron, H.N., Kemp, S. and van Kuilenburg, A.B. (2003) Histone deacetylases (HDACs): characterization of the classical HDAC family. *Biochem. J.*, **370**, 737–749.

65. Cress, W.D. and Seto, E. (2000) Histone deacetylases, transcriptional control, and cancer. *J. Cell Physiol.*, **184**, 1–16.

66. Kao, H.Y., Verdel, A., Tsai, C.C., Simon, C., Juguilon, H. and Khochbin, S. (2001) Mechanism for nucleocytoplasmic shuttling of histone deacetylase 7. *J. Biol. Chem.*, **276**, 47496–47507.

67. McKinsey, T.A., Zhang, C.L. and Olson, E.N. (2001) Identification of a signal-responsive nuclear export sequence in class II histone deacetylases. *Mol. Cell. Biol.*, **21**, 6312–6321.

68. McKinsey, T.A., Zhang, C.L., Lu, J. and Olson, E.N. (2000) Signal-dependent nuclear export of a histone deacetylase regulates muscle differentiation. *Nature*, **408**, 106–111.

69. Yoshida, M., Kijima, M., Akita, M. and Beppu, T. (1990) Potent and specific inhibition of mammalian histone deacetylase both *in vivo* and *in vitro* by trichostatin A. *J. Biol.Chem.*, **265**, 17174–17179.

70. Furumai, R., Komatsu, Y., Nishino, N., Khochbin, S., Yoshida, M. and Horinouchi, S. (2001) Potent histone deacetylase inhibitors built from trichostatin A and cyclic tetrapeptide antibiotics including trapoxin. *Proc. Natl Acad. Sci. USA*, **98**, 87–92.

71. Daniel, P., Brazier, M., Cerutti, I., Pieri, F., Tardivel, I., Desmet, G., Baillet, J. and Chany, C. (1989) Pharmacokinetic study of butyric acid administered *in vivo* as sodium and arginine butyrate salts. *Clin. Chim. Acta*, **181**, 255–263.

72. Miller, A.A., Kurschel, E., Osieka, R. and Schmidt, C.G. (1987) Clinical pharmacology of sodium butyrate in patients with acute leukemia. *Eur. J. Cancer Clin. Oncol.*, **23**, 1283–1287.

73. Gilbert, J., Baker, S.D., Bowling, M.K., Grochow, L., Figg, W.D., Zabelina, Y., Donehower, R.C. and Carducci, M.A. (2001) A phase I dose escalation and bioavailability study of oral sodium phenylbutyrate in patients with refractory solid tumor malignancies. *Clin. Cancer Res.*, **7**, 2292–2300.

74. Brusilow, S.W. and Maestri, N.E. (1996) Urea cycle disorders: diagnosis, pathophysiology, and therapy. *Adv. Pediatr.*, **43**, 127–170.

75. Berg, S., Serabe, B., Aleksic, A., Bomgaars, L., McGuffey, L., Dauser, R., Durfee, J., Nuchtern, J. and Blaney, S. (2001) Pharmacokinetics and cerebrospinal fluid penetration of phenylacetate and phenylbutyrate in the nonhuman primate. *Cancer Chemother. Pharmacol.*, **47**, 385–390.

76. Maestri, N.E., Brusilow, S.W., Clissold, D.B. and Bassett, S.S. (1996) Long-term treatment of girls with ornithine transcarbamylase deficiency. *N. Engl. J. Med.*, **335**, 855–859.

77. Mercuri, E., Bertini, E., Messina, S., Pelliccioni, M., D'Amico, A., Colitto, F., Mirabella, M., Tiziano, F.D., Vitali, T., Angelozzi, C. *et al.* (2004) Pilot trial of phenylbutyrate in spinal muscular atrophy. *Neuromuscul. Disord.*, **14**, 130–135.

78. Brahe, C., Vitali, T., Tiziano, F.D., Angelozzi, C., Pinto, A.M., Borgo, F., Moscato, U., Bertini, E., Mercuri, E. and Neri, G. (2005) Phenylbutyrate increases SMN gene expression in spinal muscular atrophy patients. *Eur. J. Hum. Genet.*, **13**, 256-259.

79. Johannessen, C.U. (2000) Mechanisms of action of valproate: a commentatory. *Neurochem. Int.*, **37**, 103–110.

80. Phiel, C.J., Zhang, F., Huang, E.Y., Guenther, M.G., Lazar, M.A. and Klein, P.S. (2001) Histone deacetylase is a direct target of valproic acid, a potent anticonvulsant, mood stabilizer, and teratogen. *J. Biol. Chem.*, **276**, 36734–36741.

81. Perucca, E. (2002) Pharmacological and therapeutic properties of valproate: a summary after 35 years of clinical experience. *CNS Drugs*, **16**, 695–714.

82. Wieser, H.G. (1991) Comparison of valproate concentrations in human plasma, CSF and brain tissue after administration of different formulations of valproate or valpromide. *Epilepsy Res.*, **9**, 154–159.

83. Khurana, T.S. and Davies, K.E. (2003) Pharmacological strategies for muscular dystrophy. *Nat. Rev. Drug Discov.*, **2**, 379–390.

84. Lunn, M.R., Root, D.E., Martino, A.M., Flaherty, S.P., Kelley, B.P., Coovert, D.D., Burghes, A.H., Thi Man, N., Morris, G.E., Zhou, J. *et al.* (2004) Indoprofen upregulates the survival motor neuron protein through a cyclooxygenase-independent mechanism. *Chem. Biol.*, **11**, 1489–1493.

85. Kelley, B.P., Lunn, M.R., Root, D.E., Flaherty, S.P., Martino, A.M. and Stockwell, B.R. (2004) A flexible data analysis tool for chemical genetic screens. *Chem. Biol.*, **11**, 1495–1503.

86. Frank-Kamenetsky, M., Zhang, X.M., Bottega, S., Guicherit, O., Wichterle, H., Dudek, H., Bumcrot, D., Wang, F.Y., Jones, S., Shulok, J. *et al.* (2002) Small-molecule modulators of Hedgehog signaling: identification and characterization of smoothened agonists and antagonists. *J. Biol.*, **1**, 10.

87. Haggarty, S.J., Koeller, K.M., Kau, T.R., Silver, P.A., Roberge, M. and Schreiber, S.L. (2003) Small molecule modulation of the human chromatid decatenation checkpoint. *Chem. Biol.*, **10**, 1267–1279.

88. Haggarty, S.J., Koeller, K.M., Wong, J.C., Butcher, R.A. and Schreiber, S.L. (2003) Multidimensional chemical genetic analysis of diversity-oriented synthesis-derived deacetylase inhibitors using cell-based assays. *Chem. Biol.*, **10**, 383–396.

89. Haggarty, S.J., Koeller, K.M., Wong, J.C., Grozinger, C.M. and Schreiber, S.L. (2003) Domain-selective small-molecule inhibitor of histone deacetylase 6 (HDAC6)-mediated tubulin deacetylation. *Proc. Natl Acad. Sci. USA*, **100**, 4389–4394.

90. Haggarty, S.J., Mayer, T.U., Miyamoto, D.T., Fathi, R., King, R.W., Mitchison, T.J. and Schreiber, S.L. (2000) Dissecting cellular processes using small molecules: identification of colchicine-like, taxol-like and other small molecules that perturb mitosis. *Chem. Biol.*, **7**, 275–286.

91. Koeller, K.M., Haggarty, S.J., Perkins, B.D., Leykin, I., Wong, J.C., Kao, M.C. and Schreiber, S.L. (2003) Chemical genetic modifier screens: small molecule trichostatin suppressors as probes of intracellular histone and tubulin acetylation. *Chem. Biol.*, **10**, 397–410.

92. Stockwell, B.R., Haggarty, S.J. and Schreiber, S.L. (1999) High-throughput screening of small molecules in miniaturized mammalian cell-based assays involving post-translational modifications. *Chem. Biol.*, **6**, 71–83.

93. Zhang, J.H., Chung, T.D. and Oldenburg, K.R. (1999) A simple statistical parameter for use in evaluation and validation of high throughput screening assays. *J. Biomol. Screen.*, **4**, 67–73.